



Simulation of soil washing with surfactants

Elaine P.S. Cheah^{a,b}, Danny D. Reible^{b,*}, Kalliat T. Valsaraj^b,
W. David Constant^c, Barry W. Walsh^a, Louis J. Thibodeaux^b

^a Department of Chemical Engineering, The University of Sydney, Sydney, New South Wales 2006, Australia

^b Hazardous Substance Research Center and Department of Chemical Engineering,

Louisiana State University, Baton Rouge, LA 70803, USA

^c Department of Civil and Environmental Engineering, Louisiana State University, Baton Rouge, LA 70803, USA

Received 20 February 1997; accepted 15 July 1997

Abstract

A mathematical model of soil washing that incorporates the surfactant enhanced mobilization and solubilization of organic compounds was implemented using a finite difference compositional reservoir simulator. The primary objective of the model was identification of the contributions of the various mechanisms—water displacement, surfactant mobilization and dissolution—on the removal of organic contaminants from soil. Mobilization of the organic phase was described by a reduction in the residual oil saturation caused by decreased interfacial tension. Increased aqueous solubility of organic compounds due to solubilization by surfactant micelles was modeled assuming local equilibrium. Parameters for the model were obtained from experimental measurements and literature sources. The model was implemented in a two-dimensional, two-phase system. Experimental data from surfactant flushing of columns contaminated with automatic transmission fluid and a mixture of chlorinated organics were used to evaluate the performance of the model. In most cases, the predicted organic recoveries were found to agree well with experimental results. For the surfactant sodium dodecyl sulfate, mobilization of organic contaminants was the main recovery mechanism for both waste liquids modeled. The results suggest that

Abbreviations: *Parameters*: g , Gravitational acceleration constant; h , Vertical coordinate; k , Intrinsic permeability tensor; k_l^1 , Relative permeability of phase 1; $K_i^{m,o}$, Mole fraction micelle–oil partition coefficient; $K_i^{m,w}$, Mole fraction micelle–water partition coefficient; $K_i^{w,o}$, Mole fraction water–oil partition coefficient; m^1 , Mass density of phase 1; P^1 , Pressure of phase 1; $P_c^{o,w}$, Oil–water capillary pressure; S^1 , Saturation of phase 1; S_r^1 , Residual saturation of phase 1; x_i^1 , Mole fraction of component i in phase 1; *Greek symbols*: ϕ , Soil porosity; μ^1 , Viscosity of phase 1; ρ^1 , Molar density of phase 1; σ , Interfacial tension (with surfactant); σ_0 , Interfacial tension at zero surfactant concentration; *Superscripts*: m, Micelle; o, Organic; oct, Octanol; w, Water

* Corresponding author.

complete dissolution of a contaminant nonaqueous phase, rather than mobilization and subsequent vertical migration, may be difficult to achieve at the surfactant concentrations studied. © 1998 Elsevier Science B.V.

Keywords: Surfactant soil washing; Mobilization; Solubilization; Nonaqueous-phase liquid

1. Introduction

Many common organic pollutants have low aqueous solubilities and high interfacial tensions with water, characteristics that render pump-and-treat remediation ineffective. Various measures have been suggested to overcome these inherent shortcomings of pump-and-treat. One of these, surfactant flushing, has long been used in the petroleum industry to increase oil recovery during the later production stages of a reservoir [1]. Surfactants can mobilize residual nonaqueous phase liquids by reducing interfacial tension, or increase organic solubility by solubilization. In oil recovery, the primary goal has been enhancing mobility to minimize surfactant usage. For environmental applications, however, mobilization of a trapped nonaqueous phase has led to concerns about further vertical migration of the displaced fluid due to gravity. As a result, the objective of surfactant addition in environmental applications has generally been to achieve essentially complete dissolution of the nonaqueous phase.

Laboratory studies of surfactant washing of contaminated soils have shown some promise. Abdul et al. [2] and Ang and Abdul [3] studied a variety of surfactants in an attempt to wash automatic transmission fluid (ATF) from a sandy soil. They concluded from batch and column washing studies that certain surfactant solutions had the potential to effectively remove nonaqueous phase liquids from soil. Soil column studies conducted by Pennell et al. [4] showed that a solution of the surfactant polyoxyethylene (20) sorbitan monooleate could considerably enhance the recovery of residual dodecane. However, mixed results have been obtained in various pilot studies. Abdul et al. [5] used a nonionic ethoxylated alcohol to remediate a site contaminated with PCBs and oils quite successfully. In contrast, the pilot tests conducted by Nash et al. [6] did not conclusively show surfactant soil washing to be a reliable remediation technology. There is a need for further research into the physics of soil washing by surfactants, especially at the field scale, before it can be fully developed into a viable in situ remediation technology.

Surfactants enhance organic contaminant recovery in soil washing through two mechanisms. First, surfactants reduce the oil–water interfacial tension and the capillary forces that trap the residual organic. As a result, the residual oil saturation in the presence of surfactant is appreciably lower, and more oil is mobilized than with simple water floods alone. Secondly, surfactants are capable of forming dynamic aggregates known as micelles. Above a critical surfactant concentration known as the critical micelle concentration (CMC), the hydrophobic end of the surfactant molecule will cluster together inside the micelle structure with the hydrophilic end exposed to the aqueous phase on the exterior. Consequently, the interior of a micelle constitutes a compatible environment for hydrophobic organic molecules; the process of incorporation of these molecules into a micelle is known as solubilization.

Below the CMC, surfactants exist in the monomeric state, and no enhancement of organic solubility is generally observed [7]. However, the aqueous solubility of certain highly hydrophobic organic compounds can be enhanced by certain surfactants even below the CMC [8], a process similar to the partitioning of highly insoluble organic compounds to the organic carbon fraction of dissolved organic macromolecules [9]. Above the CMC, the apparent solubility of hydrophobic organic compounds increases dramatically due to solubilization. For example, batch studies conducted by Pennell et al. [4] have shown that a solution of the surfactant polyoxyethylene (20) sorbitan monooleate can enhance the aqueous solubility of dodecane by six orders of magnitude.

To date, little attention has been dedicated to the mathematical modeling of soil washing by surfactants. Much of the work performed in this area has focused on the recovery of contaminants through micellar solubilization of the entrapped organic residual. Wilson [10] and Wilson and Clarke [11] presented a two-dimensional areal, single phase flow model of the solubilization process that assumes local equilibrium between the entrapped oil and micellar phases. The one-dimensional, single-phase flow model developed by Abriola et al. [12] utilized a rate-limited mass transfer process to describe surfactant solubilization, which was assumed to be the primary organic recovery mechanism. However, as noted above, solubilization is not the only process that removes organic contaminants from the subsurface upon surfactant injection. Brown et al. [13] recognized that both solubilization and mobilization could enhance organic recovery by surfactant soil washing, and incorporated both of these processes into a three-dimensional, multiphase, compositional simulator. Although the validity of this model was not assessed by any experimental data, the results of their theoretical study suggest that surfactant injection into the subsurface could enhance conventional pump-and-treat methods significantly.

In this paper, experimental data on the remediation of contaminated soil cores will be interpreted with a numerical model to test constitutive models and parameters that characterize dissolution and mobilization of organic contaminants by surfactants. The aim of this study was to evaluate the relative contributions of these processes to the enhanced organic recovery observed with surfactant soil washing. It is anticipated that the model can be applied to systems with different physical and chemical properties given adequate characterization of these properties.

2. Experimental

To assess the performance of the surfactant soil washing model, two different surfactant washing experiments were considered. In both laboratory experiments, vertical columns were packed with uncontaminated sandy silt from a local contaminated site, saturated with water and then allowed to drain by gravity for 24 h. Nonaqueous phase liquids were then pumped through the columns until breakthrough was achieved, and the columns were allowed to drain for another 24 h. In the first experiment, the column was contaminated with automatic transmission fluid (ATE) while an oily waste, a mixture of chlorinated organics from the same site as the soil, was used in the second experiment. Soil washing experiments were conducted with water and anionic sodium dodecyl

sulfate (SDS) surfactant solutions at two different concentrations of 8 mM (CMC) and 30 mM. Further details of the experimental procedure are available in Roy et al. [14,15].

3. Model development

3.1. Flow equations

Assuming that the Darcy velocity applies, two-phase (organic (o) and water (w)) flow equations in a porous media, neglecting diffusion and dispersion, can be written as:

$$\frac{\partial}{\partial t} (\phi S^l \rho^l x_i^l) = \nabla \left[\rho^l x_i^l \left(\frac{k k_r^l}{\mu^l} (\nabla P^l - m^l g \nabla h) \right) \right] \quad l = o, w; \quad i = w, \text{surf}, n_1, \dots, n_c \quad (1)$$

where ϕ is the soil porosity; S^l , ρ^l , m^l , μ^l are the saturation, molar and mass density and viscosity of phase l , respectively; x_i^l is the mole fraction of component i in phase l ; k is the intrinsic permeability tensor; P^l is the l phase pressure, g is the gravitational acceleration constant and h is the vertical coordinate. The $n_c + 2$ system components are water (w), surfactant (surf), and n_c organic compounds. The equations represented by Eq. (1) are coupled via the relative permeability, k_r^l and capillary pressure, $P_c^{o,w}$, which are generally written as functions of water saturation, S^w :

$$k_r^w = f_1(S^w) \quad (2a)$$

$$k_r^o = f_2(S^w) \quad (2b)$$

$$P_c^{o,w} = P^o - P^w = g(S^w) \quad (3)$$

These constitutive relationships are strong functions of surfactant concentration, as described in Section 3.2.

Eqs. (1), (2a), (2b) and (3), together with the constraint equations:

$$\sum_i x_i^l = 1 \quad l = o, w \quad (4)$$

$$\sum_l S^l = 1 \quad (5)$$

constitute a system of highly nonlinear coupled partial differential equations which represents a general framework for the modeling of surfactant enhanced soil washing.

3.2. Mobilization

Mobilization of nonaqueous phase liquids by surfactants is caused by a reduction in interfacial tension leading to decreased residual oil saturation and capillary pressure, and an increased oil relative permeability. The effect of surfactants on the oil permeability and residual saturation was modeled by relative permeability curves that were allowed to vary with surfactant concentration and hence interfacial tension. At zero surfactant

concentration, oil–water relative permeability curves were represented by Corey-type imbibition equations for poorly sorted unconsolidated sand [16]:

$$k_{r(\sigma 0)}^w = \left(\frac{S_{(\sigma 0)}^w - S_{r(\sigma 0)}^w}{1 - S_{r(\sigma 0)}^w} \right)^{3.5} \quad (6a)$$

$$k_{r(\sigma 0)}^o = \left[1 - \frac{S_{(\sigma 0)}^w - S_{r(\sigma 0)}^w}{1 - S_{r(\sigma 0)}^w - S_{r(\sigma 0)}^o} \right]^2 \left[1 - \left(\frac{S_{(\sigma 0)}^w - S_{r(\sigma 0)}^w}{1 - S_{r(\sigma 0)}^w - S_{r(\sigma 0)}^o} \right)^{1.5} \right] \quad (6b)$$

where $\sigma 0$ designates the interfacial tension at zero surfactant concentration. $k_{r(\sigma 0)}^w$ and $k_{r(\sigma 0)}^o$ are respectively the water and oil relative permeabilities corresponding to an interfacial tension of $\sigma 0$; $S_{r(\sigma 0)}^w$ and $S_{r(\sigma 0)}^o$ are the residual water and oil saturations respectively and $S_{(\sigma 0)}^w$ is the water saturation.

The relative permeability curves in the presence of surfactant were modeled using an approach similar to Amaefule and Handy [17]:

$$k_{r(\sigma)}^w = \left(\frac{S_{(\sigma)}^w - S_{r(\sigma)}^w}{1 - S_{r(\sigma)}^w} \right) \left\{ 3.2 S_{r(\sigma)}^w \left[\left(\frac{S_{(\sigma)}^w - S_{r(\sigma)}^w}{1 - S_{r(\sigma)}^w} \right)^2 - 1 \right] + 1 \right\} \quad (7a)$$

$$k_{r(\sigma)}^o = \left(1 - \frac{S_{(\sigma)}^w - S_{r(\sigma)}^w}{1 - S_{r(\sigma)}^w - S_{r(\sigma)}^o} \right) \left\{ 5 S_{r(\sigma)}^o \left[\left(1 - \frac{S_{(\sigma)}^w - S_{r(\sigma)}^w}{1 - S_{r(\sigma)}^w - S_{r(\sigma)}^o} \right) - 1 \right] + 1 \right\} \quad (7b)$$

where the subscript σ designates that a quantity is evaluated at an interfacial tension of σ corresponding to a particular surfactant concentration. Hence, $S_{r(\sigma)}^w$ and $S_{r(\sigma)}^o$ are, respectively, the residual water and organic saturations at an interfacial tension of σ and $S_{(\sigma)}^w$ is the corresponding water saturation.

Capillary pressure is also a strong function of surfactant concentration. At a given saturation, the capillary pressure decreases as the oil–water interfacial tension decreases with increased surfactant concentration up to the CMC. The oil–water capillary pressure–saturation curve at zero surfactant concentration was modified (to account for differences in porous medium properties) from Slider [18]. Using Leverett's J -function [18], capillary pressure was obtained as a function of interfacial tension, which, in turn, is a function of surfactant concentration:

$$P_{c(\sigma)}^{o,w} = P_{c(\sigma 0)}^{o,w} \frac{\sigma}{\sigma 0} \quad (8)$$

3.3. Solubilization

In this study, the enhancement of organic solubility by surfactant at concentrations below the CMC was assumed to be negligible. Above the CMC, organic phase solubilization was assumed to occur via an equilibrium process. The micelles formed above the CMC can be thought of as a pseudophase with a certain capacity for organic

components. This capacity is related to the organic-phase concentration by a micelle–oil partition coefficient, $K_i^{m,o}$:

$$x_i^m = K_i^{m,o} x_i^o \quad i = n_1, \dots, n_c \quad (9)$$

where x_i^m and x_i^o are the mole fractions of component i in the micellar and organic phases, respectively.

The micelle–oil partition coefficient, $K_i^{m,o}$ can be expressed as

$$K_i^{m,o} = \frac{x_i^m}{x_i^w} \frac{x_i^w}{x_i^o} = K_i^{m,w} \cdot K_i^{w,o} \quad i = n_1, \dots, n_c \quad (10)$$

The second term in Eq. (10) is simply the water–oil partition coefficient, which was approximated as:

$$K_i^{w,o} = x_i^{w,sol} \quad i = n_1, \dots, n_c \quad (11)$$

where $x_i^{w,sol}$ is the solubility of i in pure water. The first term in Eq. (10), the micelle–water partition coefficient, $K_i^{m,w}$ has been correlated to the octanol–water partition coefficient by various researchers [19–21]. In this study, the correlation of Valsaraj and Thibodeaux [22] was used to calculate the micelle–water partition coefficient as

$$\log K_i^{m,w} = 0.858 \log K_i^{oct,w} - 0.017 \quad i = n_1, \dots, n_c \quad (12)$$

where $K_i^{oct,w}$ is the octanol–water partition coefficient.

4. Method

All simulations were performed using STARS [23], a three-dimensional, finite-difference, multicomponent, three-phase compositional reservoir simulator. STARS is capable of simulating a wide range of chemical and physical reservoir processes like steam injection, fireflood and dry and wet combustion by solving the flow equations (Eqs. (1), (2a), (2b), (3)–(5)) implicitly using incomplete Gaussian elimination. In this study, STARS was adjusted to allow the simulation of mobilization and solubilization processes.

4.1. Grid

For both ATF and oily waste simulations, the soil column was simulated by a vertical two-dimensional homogeneous grid. The porosity and absolute permeability of this grid were set at the experimental average values [14,15], as tabulated in Tables 1 and 2. A constant pressure boundary condition was imposed on the column outlet. Water or SDS solution was injected into the column at the experimental flow rates (Tables 1 and 2).

4.2. Initial conditions

The column was initially water-saturated. In both ATF and oily waste simulations, the initial oil distribution in the column was determined from a simulation of the oil contamination and drainage process; this distribution was found to be largely determined

Table 1
Parameters of ATF water and surfactant washing simulations

Parameter	Water run	Surfactant runs	Reference
Soil permeability (md)	137	137	[15]
Soil porosity	0.45	0.45	[15]
Water–oil partition coefficient (mole fraction ratio)	2.7×10^{-6}	2.7×10^{-6}	Calculated assuming maximum ATF aqueous solubility of 50 mg/l [15]
Micelle–oil partition coefficient (mole fraction ratio)	–	0.006	Calculated from Refs. [15,22]
Organic phase density (g/cm ³)	0.875	0.875	[15]
Organic phase viscosity (cp)	52.5	52.5	[24]
Residual water saturation	0.30	0.30 ($C_{\text{surf}} = 0$)	[25]
Residual oil saturation	0.29	0.30 ($C_{\text{surf}} = \text{CMC and above}$)	Fitted
		0.20 ($C_{\text{surf}} = \text{CMC and above}$)	Fitted
Initial oil mass in column (g)	43.8	55.1 (8 mM)	R.R. Kommalapati, personal communication, 1996.
		53.3 (30 mM)	R.R. Kommalapati, personal communication, 1996.
Water/SDS injection rate (cm ³ /min)	2.6	2.6	[15]

C_{surf} : surfactant concentration.

Table 2
Parameters of oily waste water and surfactant washing simulations

Parameter	Water run ^a	Surfactant runs ^{a,b}	Reference
Soil permeability (md)	171	171	[14]
Soil porosity	0.40	0.40	[14]
Components (mole %)	TCE (6.2%)	TCE (6.2%)	[26]
	TCA (0.7%)	TCA (0.7%)	
	DNAPL (93.1%)	DNAPL (93.1%)	
Water–oil partition coefficient (mole fraction ratio)	5.9×10^{-4} (TCE)	5.9×10^{-4} (TCE)	Calculated from Ref. [14]
	3.1×10^{-4} (TCA)	3.1×10^{-4} (TCA)	
	0 (DNAPL)	0 (DNAPL)	
Organic phase density (g/cm ³)	1.33	1.33	[14]
Organic phase viscosity (cp)	58.8	58.8	[14]
Residual water saturation	0.30	0.30 ($C_{\text{surf}} = 0$)	[25]
		0.30 ($C_{\text{surf}} = \text{CMC and above}$)	fitted
Residual oil saturation	0.15	0.15 ($C_{\text{surf}} = 0$)	fitted
		0.10 ($C_{\text{surf}} = \text{CMC and above}$)	fitted
Initial oil volume in column (cm ³)	40.6	31.7 (8 mM)	[26]
		36.6 (30 mM)	[26]
Water/SDS injection rate (cm ³ /min)	2.6	2.6	[14]

^aTCE: 1,1,2-trichloroethane; TCA: 1,1,2,2-tetrachloroethane; DNAPL: insoluble fraction of oily waste.

^b C_{surf} : surfactant concentration.

by a balance between the capillary and gravitational forces acting on the nonaqueous phase liquid globules.

4.3. Component properties

Both ATF and the oily waste are complex mixtures with poorly characterized properties. ATF is a light nonaqueous phase liquid of low solubility and volatility that contains mainly long chain petroleum hydrocarbons [3]. To simplify the model, ATF was simulated as a single compound with the properties tabulated in Table 1.

The oily waste is a highly viscous, dense nonaqueous phase liquid that contains volatile and soluble compounds. The main identifiable constituents, comprising 17 wt.% of the oily waste, were 1,1,2-trichloroethane, 1,1,2,2-tetrachloroethane, tetrachlorethylene, hexachlorobenzene and hexachlorobutadiene [26]. Due to their high water solubility, 1,1,2-trichloroethane (TCE) and 1,1,2,2-tetrachloroethane (TCA) were simulated separately in the oily waste simulations. The rest of the oily waste, a mixture of low solubility halo- and hydrocarbon compounds [26], was simulated using a water insoluble pseudo-component of average waste properties (DNAPL). A summary of the components and their properties used in the oily waste simulations is given in Table 2.

4.4. Parameter evaluation

4.4.1. Soil–fluid properties

Based on its soil texture, the field capacity moisture content of the sandy silt in both experiments would be approximately 12% of the total soil volume [25]. Using the

porosities in Tables 1 and 2, the corresponding water saturation would be roughly 0.3. The residual water saturation in the absence of surfactant was thus set at 0.30 for both ATF and oily waste simulations. In each case, the residual organic saturation at zero surfactant concentration was set by matching the respective water flooding recovery curves; the final values used are given in Tables 1 and 2. These values are in the range of residual organic saturations reported by Wilson et al. [27] for the saturated zone.

The residual water and oil saturations in the presence of a surfactant, which were fitted to the experimental data, are shown in Tables 1 and 2. These saturations can be estimated through direct experimental measurements. Alternatively, residual saturations have been related to interfacial tension and hence surfactant concentration using the capillary number [17,28]. The latter approach was used with experimentally measured interfacial tensions at SDS concentrations of 0 and 30 mM to validate the residual saturation values of the model. Since interfacial tension is constant above the CMC, the value measured at the 30 mM SDS concentration was assumed to be representative of the interfacial tension at the CMC.

With an experimentally determined reduction in ATF–water interfacial tensions of approximately two orders of magnitude (from 8.0 mN/m at zero SDS concentration to 0.07 mN/m for a SDS concentration at or above the CMC), the corresponding decrease in the residual ATF saturation was evaluated using the correlation of Amaefule and Handy [17] to be by a factor of approximately 0.77. Assuming that the calibrated residual ATF saturation at zero SDS concentration is 0.29 (Table 1), the residual ATF saturation at the CMC and above would be 0.22. In comparison, the corresponding fitted value of 0.20 (Table 1) agrees quite well. For the same SDS concentration range, the correlation of Amaefule and Handy [17] predicted a decrease in the residual water saturation by a factor of 0.93, giving a residual water saturation of 0.28 assuming a residual water saturation of 0.30 in the absence of SDS (Table 1). Again, the predicted value agrees well with the experimentally fitted residual water saturation of 0.30 (Table 1). Due to the hazardous nature and experimental difficulties associated with the oily waste [29], interfacial tension measurements were not attempted, and the residuals in this case could not be similarly validated.

4.4.2. Solubilization parameters

Based on the maximum solubility of ATF in water, the ATF water–oil partition coefficient was approximately 2.7×10^{-6} (Table 1). Using Eq. (12), the micelle–water partition coefficient for ATF was found to be approximately 2.3×10^3 giving a micelle–oil partition constant of 0.006. A comparison of the water–oil and micelle–oil partition coefficients for ATF (Table 1) shows that SDS can enhance the equilibrium solubility of ATF significantly.

5. Results and discussion

5.1. Water flushing

Fig. 1 shows ATF and oily waste recoveries after water flushing. The error bars in this and subsequent figures are the experimental standard deviation. The simulated water

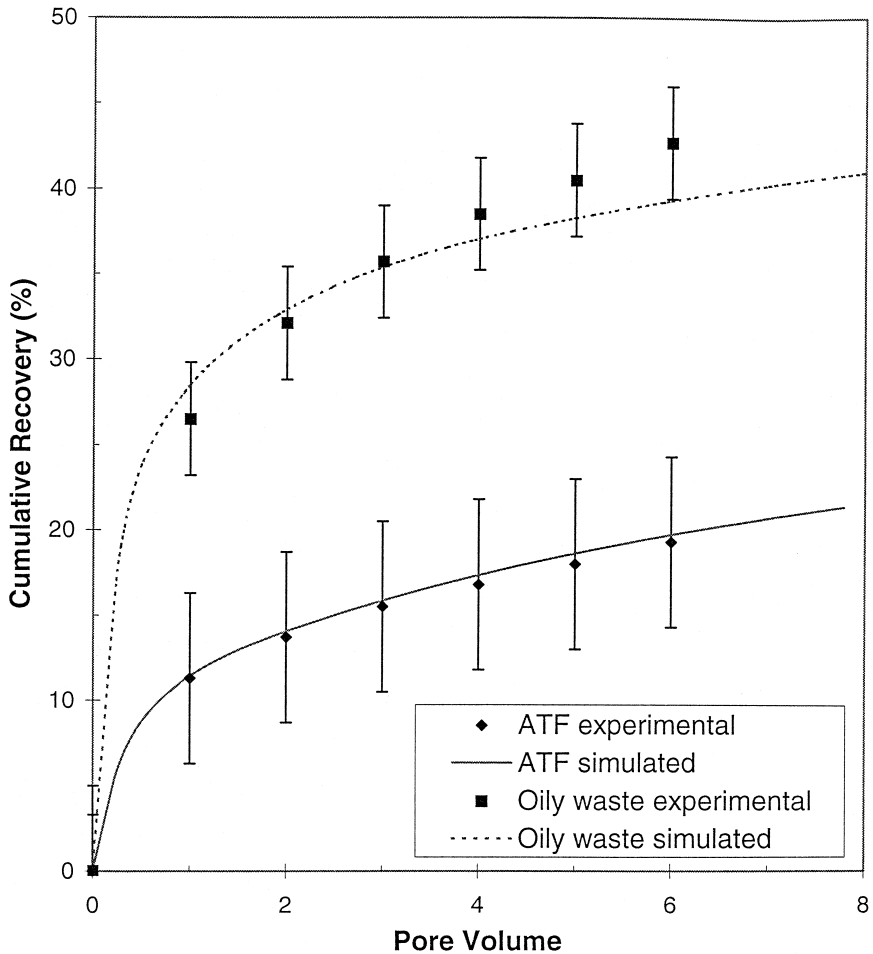


Fig. 1. ATF and oily waste recovery due to displacement of contaminant by water flushing.

recovery curves show reasonable agreement with the experimental data points. Since the oily waste is of a higher density than water, gravity forces resulted in an essentially saturated pool of waste at the base of the column before flushing. Consequently, water flushing resulted in much higher initial recoveries of waste compared to ATF. Modeling of column drainage before initiation of the displacement experiment was required to define the initial conditions in the column properly, and to accurately predict the resulting displacement curves.

Approximately 32% of the ATF present in the column initially was above residual organic saturation. The cumulative ATF recovery of 19% at the end of water flooding is due to the displacement of a portion of this free-phase material present above residual saturation. Similarly, water recovery of the oily waste is through the displacement of free-phase liquid that comprised 54% of the waste present initially. For a system

containing oil at residual saturation, the expected recovery under water flushing would be negligible.

5.2. Surfactant washing: Automatic transmission fluid

The experimental and simulated ATF recoveries for SDS washing at the CMC (8 mM) and 30 mM are shown in Figs. 2 and 3, respectively. The two predicted recovery curves in Fig. 2 differ, in that one of the curves take solubilization into account (solid curve) in addition to displacement and mobilization (dashed curve). The 8 mM simulated curves agree to within one standard deviation of the experimental values except for the initial point. This may imply that the initial modeled oil distribution in this case did not provide an adequate description of the experimental distribution. Fig. 2 shows that

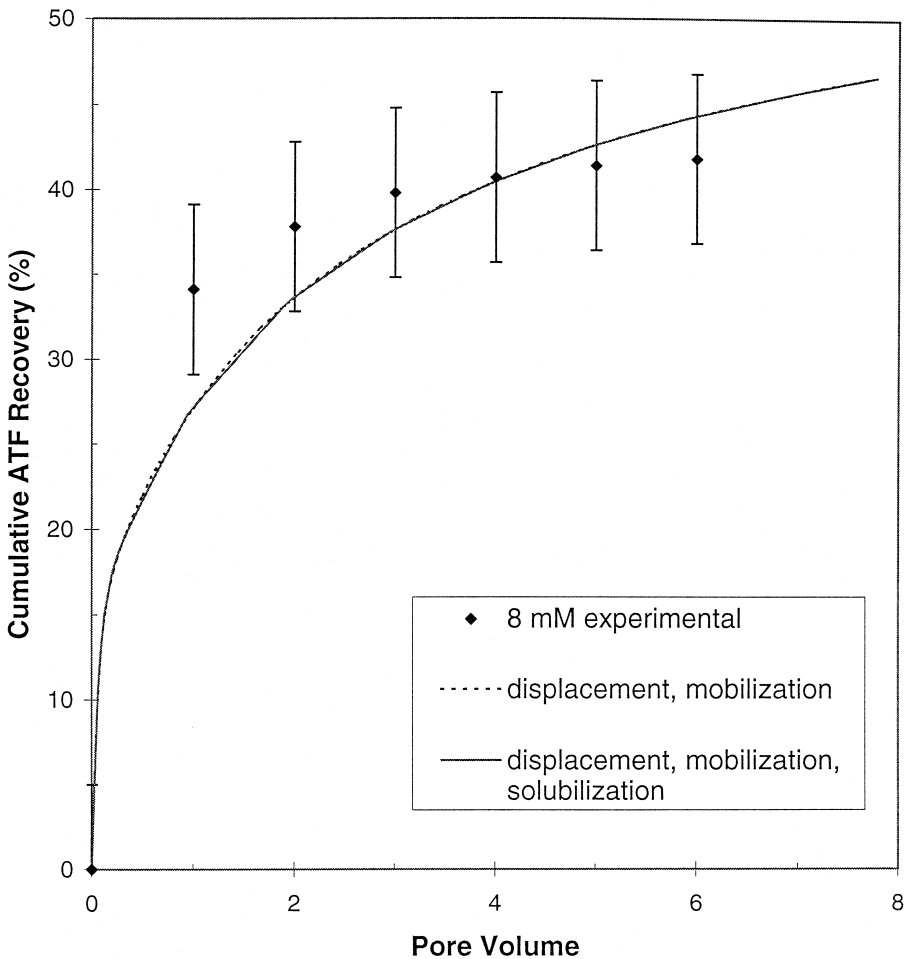


Fig. 2. ATF recovery due to displacement, mobilization and solubilization by 8 mM SDS.

the enhanced recovery observed with SDS washing at the CMC can mainly be accounted for by the reduction in the oil–water interfacial tension causing mobilization of ATF. There is virtually no additional recovery when solubilization is included at this concentration. Consistent with this conclusion is the observation of a flattening of the percent recovery curve beyond 3 pore volumes of washing fluid. At the CMC, micelles are just beginning to form. Thus, the number of micelles in solution is small and the enhancement due to solubilization of organic compounds into the micellar phase is correspondingly low.

Fig. 3 shows ATF recovery when the soil column is washed with SDS at a concentration of 30 mM. Again, enhanced recovery of ATF is due to mobilization of the contaminant as the interfacial tension is reduced by SDS. The incremental recovery due to micellar solubilization is small, approximately 2 to 3% at the last experimental point. Solubilization involves the incorporation of organic molecules into the interior of

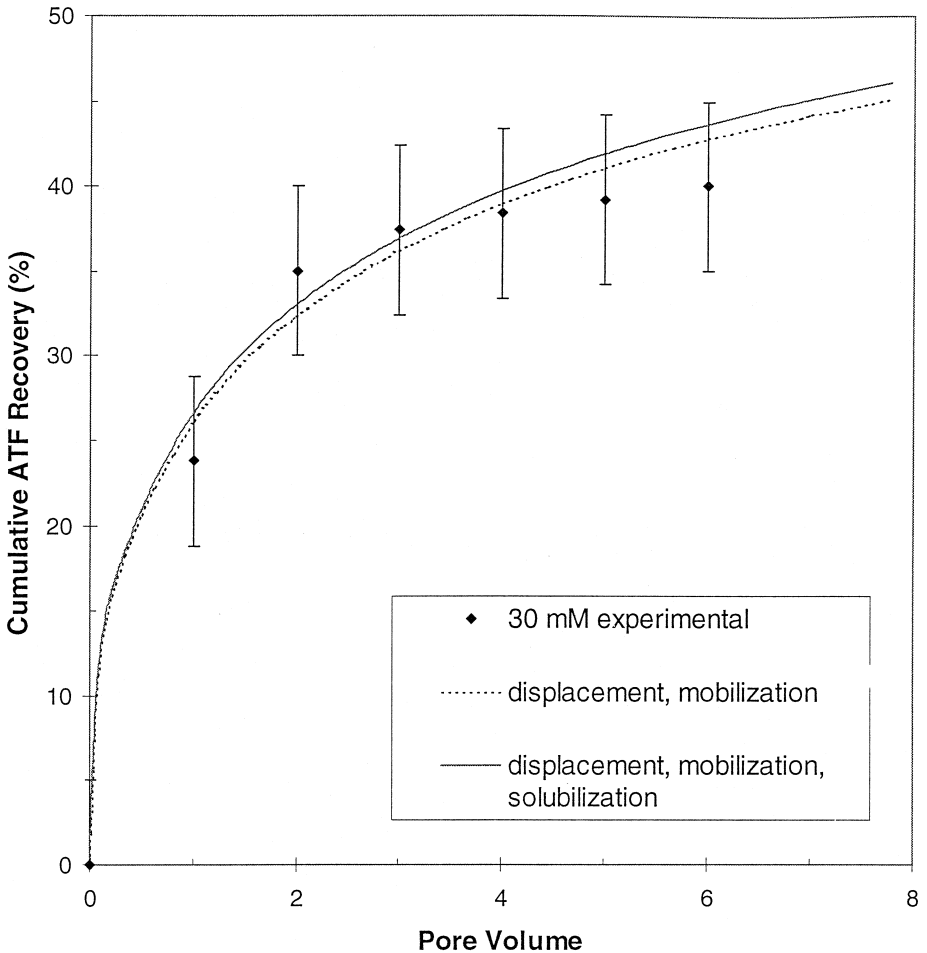


Fig. 3. ATF recovery due to displacement, mobilization and solubilization by 30 mM SDS.

surfactant micelles. Above the CMC, the number of micelles increases with surfactant concentration. Therefore, solubilization would be expected to increase with surfactant concentration above the CMC. However, an almost threefold increase in the number of micelles in the aqueous phase has not increased ATF recovery significantly, implying that solubilization is a relatively less important mechanism in the SDS-enhanced recovery of ATF.

5.3. Surfactant washing: Oily waste

Fig. 4 shows that similar to ATF, the experimental 8 and 30 mM oily waste recovery curves were not significantly different. It was therefore assumed that solubilization played only a minor role in enhancing oily waste recovery by SDS flushing, and was consequently not simulated. At both SDS concentrations, the enhanced recoveries observed under surfactant washing can be explained mainly by mobilization of the oily

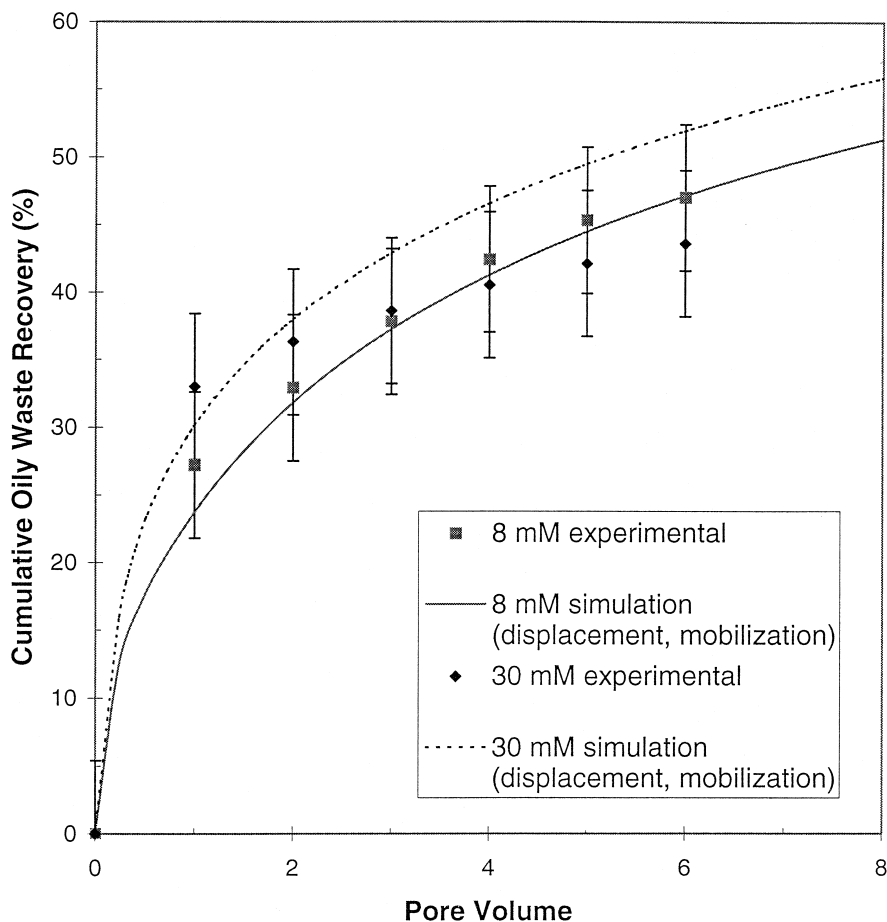


Fig. 4. Oily waste recovery due to displacement and mobilization by 8 and 30 mM SDS.

waste. Fig. 4 compares the experimental and predicted oily waste recoveries due to displacement by water and mobilization by SDS. The predicted recovery using 8 mM SDS compares very well with the experimental values. In the 30 mM case, the agreement between the simulated and experimental values was poor. After approximately 3.5 pore volumes, the simulated recovery exceeded the experimental values by more than one standard deviation. A closer examination of the experimental oily waste recovery with 30 mM SDS shows that the recovery curve has an anomalously low slope and actually intersects the 8 mM recovery curve. This may indicate an experimentally inefficient sweep of the column due to low permeability zones, with the ultimate recovery determined by the accessibility of the surfactant to these zones. Some degree of this phenomenon is suggested in all experiments, in that the observed recoveries increase more slowly than the prediction after 2 pore volumes in most simulations. The anomalous behavior of the 30 mM experiment may also be the result of unknown differences in the initial and modeled oily waste distributions in the column.

In both ATF and oily waste experiments, mobilization appears to be the main mechanism by which sodium dodecyl sulfate enhances nonaqueous phase liquid recovery. Even under the assumption of local equilibrium between the organic and aqueous phases, the incremental recovery due to solubilization is minimal, and cannot explain the enhanced recovery observed with SDS. The dissolution of a nonaqueous phase due to micellar solubilization appears to be a less efficient recovery mechanism compared to organic phase mobilization at the SDS concentrations studied. To predict the effect of SDS soil washing, an estimate of interfacial tension variation with surfactant concentration is required to quantify residual organic saturation.

The surfactant recovery curves for both ATF and oily waste appear to approach an asymptote with time (Figs. 2–4). This may be an indication that the ultimate recoveries were limited by low permeability zones within the column. This effect would not have been predicted by the homogeneous soil column model used, leading to an overprediction of ultimate organic recoveries, as observed in Figs. 2–4.

Previous studies [4,30] have reported surfactant loss from the aqueous phase due to sorption onto the soil, a process that has generally been modeled using adsorption isotherms [11,13]. In this study, no attempt was made to describe soil–surfactant sorption since repulsion between the anionic SDS molecules and the negatively charged clay particles of the soil is expected to minimize their interaction. If required, modifications to the model to simulate the sorption process can be accommodated with ease, given experimentally determined sorption parameters.

6. Conclusions

This study has shown that the laboratory scale surfactant washing of soil contaminated by both light and dense phase organics can be adequately simulated using simple constitutive relations commonly employed to model fluid flow in soil. It is conceivable that the model presented here can be applied to different surfactant soil washing studies given adequate characterization of the physical and chemical properties of these systems.

Water flushing can only displace organic phase present above residual saturation from a contaminated soil matrix, and is therefore expected to be of limited effectiveness

in remediating soils containing organic contaminants of low aqueous solubility at near residual saturations.

Surfactant soil washing using sodium dodecyl sulfate results in enhanced organic contaminant recovery that can be explained by mobilization of these organics due to the reduction in the oil–water interfacial tension and residual organic saturation. This effect can be modeled by constitutive relationships that are functions of surfactant concentration; and thus, oil–water interfacial tension.

In both sodium dodecyl sulfate flushing experiments modeled, solubilization was a minor recovery mechanism and did not account for any significant removal of contaminant from the soil column even under the assumption of local equilibrium. Because in situ soil washing with surfactants may result in mobilization and vertical migration of dense nonaqueous phase liquids, solubilization is generally the preferred mechanism of contaminant removal. The negligible solubilization observed in this study suggests that achieving this goal may be difficult with the surfactant and wastes employed herein.

Acknowledgements

The partial support of NSF-EPSCoR (1992-1996) ADP-03, the US District Court, Middle District of Louisiana, through the Louisiana State University Hazardous Waste Research Center and the Hazardous Substance Research Center S/SW, is acknowledged.

References

- [1] L.W. Lake, *Enhanced Oil Recovery*, 1st edn., Prentice-Hall, Englewood Cliffs, NJ, 1989, pp. 354–416.
- [2] A.S. Abdul, T.L. Gibson, D.N. Rai, *Ground Water* 28 (1990) 920.
- [3] C.C. Ang, A.S. Abdul, *Ground Water Monogr. Rev.* 11 (1991) 121.
- [4] K.D. Pennell, L.M. Abriola, W.J. Weber Jr., *Environ. Sci. Technol.* 27 (1993) 2332.
- [5] A.S. Abdul, T.L. Gibson, C.C. Ang, J.C. Smith, R.E. Sobczynski, *Ground Water* 30 (1992) 219.
- [6] J. Nash, R.P. Traver, D.C. Downey, *Surfactant-enhanced in situ soils washing*, Engineering and Services Laboratory, Air Force Engineering and Services Center, Tyndall Air Force Base, Florida, Report No. ESL-TR-87-18, 1987, pp. 41–42.
- [7] P.C. Hiemenz, *Principles of Colloid and Surface Chemistry*, 2nd edn., Marcel Dekker, New York, 1986, p. 448.
- [8] D.E. Kile, C.T. Chiou, *Environ. Sci. Technol.* 23 (1989) 832.
- [9] C.T. Chiou, D.E. Kile, T.I. Brinton, R.L. Malcolm, J.A. Leenheer, P. MacCarthy, *Environ. Sci. Technol.* 21 (1987) 1231.
- [10] D.J. Wilson, *Sep. Sci. Technol.* 24 (1989) 863.
- [11] D.J. Wilson, A.N. Clarke, *Sep. Sci. Technol.* 26 (1991) 1177.
- [12] L.M. Abriola, T.J. Dekker, K.D. Pennell, *Environ. Sci. Technol.* 27 (1993) 2351.
- [13] C.L. Brown, G.A. Pope, L.M. Abriola, K. Sepehrnoori, *Water Resour. Res.* 30 (1994) 2959.
- [14] D. Roy, K.T. Valsaraj, W.D. Constant, M. Darji, *J. Hazard. Mater.* 38 (1994) 127.
- [15] D. Roy, R.R. Kommalapati, K.T. Valsaraj, W.D. Constant, *Water Res.* 29 (1995) 589.
- [16] R.A. Greenkorn, *Flow Phenomena in Porous Media: Fundamentals and Applications in Petroleum, Water and Food Production*, 1st edn., Marcel Dekker, New York, 1983, p. 130.
- [17] J.O. Amaefule, L.L. Handy, *Soc. Petrol. Eng. J.* 22 (1982) 371.

- [18] H.C. Slider, *Practical Petroleum Reservoir Engineering Methods*, 1st edn., Petroleum Publishing, Tulsa, 1976, pp. 273–283.
- [19] J.L. Collett, L. Koo, *J. Pharm. Sci.* 64 (1975) 1253.
- [20] E. Azaz, M. Donbrow, *J. Colloid Interface Sci.* 57 (1976) 11.
- [21] K.T. Valsaraj, A. Gupta, L.J. Thibodeaux, D.P. Harrison, *Water Res.* 22 (1988) 1173.
- [22] K.T. Valsaraj, L.J. Thibodeaux, *Water Res.* 23 (1989) 183.
- [23] Computer Modelling Group, *STARS Steam and Additive Reservoir Simulator: Gas, Solvent and Aqueous Additives, Version 96 User's Guide*, Computer Modelling Group, Calgary, 1996.
- [24] D.V. Doshi, *Modeling vertical migration of non-aqueous phase liquid wastes in unsaturated soils*, PhD dissertation, Louisiana State Univ., Baton Rouge, LA, 1994.
- [25] W.J. Lyman, P.J. Reidy, B.J. Levy, *Assessing UST corrective action technology: A scientific evaluation of the mobility and degradability of organic contaminants in subsurface environments*, Risk Reduction Engineering Laboratory, Office of Research and Development, US Environmental Protection Agency, Cincinnati, OH, Report No. EPA/600/2-91/053, 1991, p. 306.
- [26] M. Darji, *Removal of hazardous oily waste from soil matrix under different flow conditions*, MS thesis, Louisiana State Univ., Baton Rouge, LA, 1993.
- [27] J.L. Wilson, S.H. Conrad, W.R. Mason, W. Peplinski, E. Hagan, *Laboratory investigation of residual liquid organics from spills, leaks and the disposal of hazardous wastes in ground water*, Robert S. Kerr Environmental Research Laboratory, Office of Research and Development, US Environmental Protection Agency, Ada, OK, Report No. EPA/600/6-90/004, 1990, pp. 143–163.
- [28] I. Chatzis, N.R. Morrow, *Soc. Petrol. Eng. J.* 24 (1984) 555.
- [29] S.R. Kurkal, P.A. Schenewerk, J.M. Wolcott, in: D.W. Tedder, F.G. Pohland (Eds.), *Emerging Technologies in Hazardous Waste Management VI*, American Academy of Environmental Engineers, 1996, p. 106.
- [30] Z. Adeel, R.G. Luthy, *Environ. Sci. Technol.* 29 (1995) 1032.